ChemPubSoc Europe

DOI: 10.1002/cssc.201300363

Ligand Effects on the Hydrogenation of Biomass-Inspired Substrates with Bifunctional Ru, Ir, and Rh Complexes

Eveline Jansen,[a] Linda S. Jongbloed,[a] Dorette S. Tromp,[a] Martin Lutz,[b] Bas de Bruin,[a] and Cornelis J. Elsevier*[a]

We herein report on the application and structural investigation of a new set of complexes that contain bidentate N-heterocyclic carbenes (NHCs) and primary amine moieties of the type [M(arene)Cl(L)] [M = Ru, Ir, or Rh; arene = *p*-cymene or pentamethylcyclopentadienyl; L = 1-(2-aminophenyl)-3-(*n*-alkyl)imidazol-2-ylidine]. These complexes were tested and compared in the hydrogenation of acetophenone with hydrogen. Structural variations in the chelate ring size of the heteroditopic ligand revealed that smaller chelate ring sizes in combination with ring conjugation in the ligand are beneficial for the activity of this type of catalyst, favoring an inner-sphere coordination pathway. Additionally, increasing the steric bulk of the alkyl substituent on the NHC aided the reaction, showing almost no induction period and formation of a more active catalyst for the *n*-butyl complex relative to complexes with smaller Me and Et substituents. As is common in hydrogenation reactions, the activity of the complexes decreases in the order Ru > Ir > Rh. The application of [Ru(*p*-cym)Cl(L)]PF_6, which outperforms its reported analogues, has been successfully extended to the hydrogenation of more challenging biomass-inspired substrates.

Introduction

Environmental issues and depletion of fossil-fuel reserves are stimulating society to develop renewable sources of energy and materials:[1–3] sources that are either abundantly available or replaceable. The current feedstock of choice when it comes to finding a renewable carbon source is biomass (i.e., indirectly CO_2). In addition to converting biomass into alternative fuels, this feedstock can be used to render many other processes sustainable. In light of these developments a set of key intermediates (platform molecules) originating from processed biomass has been defined.[4] These can be transformed into a large selection of valuable products. To achieve this, methods for the re- and defunctionalization of biogenic substrates have to be developed and optimized, creating a toolkit filled with selective catalytic conversions that a chemist can use to create the desired product.[5,6] For the pharmaceutical industry this predominantly means development of homogeneously catalyzed conversions because the mild conditions associated with these processes characteristically allow for the retention of natural complexity or incorporation of difficult functionalities in a molecule.

N-Heterocyclic carbenes (NHCs) have already found widespread use in many catalytic conversions, including those concerning biomass. The research groups of Marr,[7] Crabtree,[8] Yamaguchi,[9] and Peris[10] produced metal–NHC complexes that were shown to be applicable for the conversion of platform chemicals or biomass-inspired substrates. The hydrogenation of oxygenates, such as ketones, esters, and similarly functionalized compounds using molecular hydrogen, is an attractive green process,[11] and an attractive method to convert biomass into useful chemicals. Especially, the discovery of the NH-effect by Noyori et al.[12] provided a breakthrough in these hydrogenation reactions. This bifunctional mechanism is proposed to proceed in the outer coordination sphere, where an NH moiety activates, for example, a carbonyl-containing substrate through a NH···O=C hydrogen bond, which preorganizes and facilitates the attack of the carbonyl group by the metal hydride in a pericyclic six-membered transition state.[13,14] Since that discovery, bifunctional catalysts have played a key role in several pioneering reports on polar bond hydrogenation reactions, most notably by the research groups of Noyori,[15] Morris,[16] Clarke,[17] and Milstein.[18]

In our design of new ligands for carbonyl-group hydrogenation reactions, we decided to combine a NHC moiety, providing favorable donating properties widely used in hydrogenation reactions,[19] with an amine functionality possibly allowing bifunctional substrate activation.[20,21] In general, the use of ligands that contain NHC and primary amine groups in coordination chemistry is thus far poorly developed and only a few transition-metal-based catalysts based on this motif have been

[a] *E. Jansen, L. S. Jongbloed, Dr. D. S. Tromp, Prof. Dr. B. de Bruin, Prof. Dr. C. J. Elsevier*
van 't Hoff Institute for Molecular Chemistry
University of Amsterdam
Science Park 904, 1098 XH Amsterdam (The Netherlands)
E-mail: c.j.elsevier@uva.nl

[b] *Dr. M. Lutz*
Crystal and Structural Chemistry
Bijvoet Center for Biomolecular Research
Utrecht University
Padualaan 8, 3584 CH Utrecht (The Netherlands)

Supporting Information for this article is available on the WWW under http://dx.doi.org/10.1002/cssc.201300363.

developed to date.[22–25] The field is, however, rapidly developing due to the promising results obtained with this ligand scaffold thus far. Hence, to develop new tools for efficient conversion of biomass-derived platform molecules and model substrates thereof, we synthesized a set of new NHC–amine ligands and used these to prepare a set of group 8 and 9 transition-metal complexes of general structure I (Figure 1).

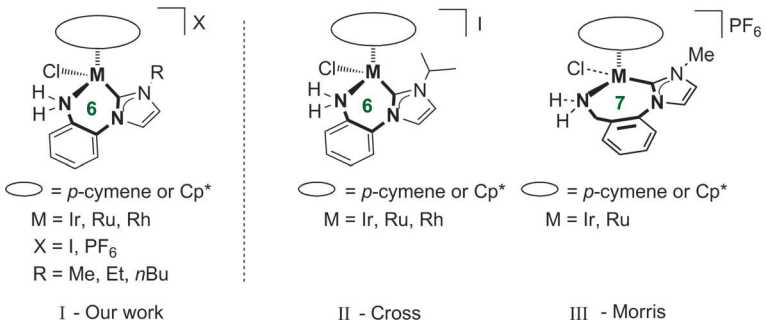

Figure 1. General structures of half-sandwich complexes synthesized herein (I), and by the groups of Cross (II)[22] and Morris (III)[25–28].

An analogous NHC–amine complex (Figure 1, structure III) was previously reported by Morris et al.,[25–28] but differs on two distinct points: the chelate ring that is formed is larger and the electronic structure lacks the conjugation with the amine function present in our ligand. They performed extensive DFT studies on the performance of the catalyst in, among others, the H_2-hydrogenation of ketones, which laid a firm foundation in understanding the basics of the reaction. During the course of our investigation Cross et al.[22] reported a similar complex (Figure 1, structure II), but until now they only tested transfer hydrogenation reactions.[26–28]

Morris et al.[27] showed that, based on DFT calculations, a [Ru(*p*-cym)(L)] complex (*p*-cym = *p*-cymene, L = NHC–amine-type ligand) in the H_2-hydrogenation of acetophenone favors an inner-sphere bifunctional mechanism, whereas a pentamethylcyclopentadienyl (Cp*) substituent facilitates a much faster

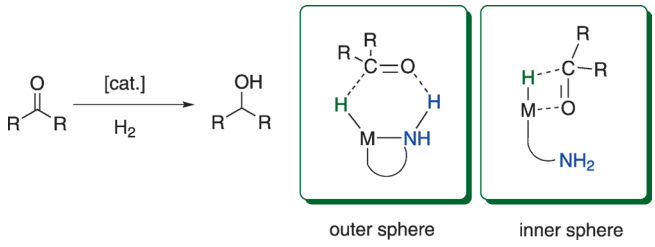

Figure 2. Principle of carbonyl hydrogenation by H_2. Two possible transition states for hydride transfer are shown: outer-sphere bifunctional mechanism (left) and direct inner-sphere mechanism (right).

outer-sphere bifunctional mechanism (Figure 2). In the H_2-hydrogenation of acetophenone turnover frequencies (TOFs) of 213 and 10800 h^{-1} for [Ru(*p*-cym)(L)] and [RuCp*(L)], respectively, have been reported.[26,27] Building on this work, we investigated the effect of structural variations of the catalyst on catalytic activity in H_2-hydrogenation of ketones in more detail. In general, the activity of a catalyst is closely related to its structure: a small structural change can bring about large differences in activity and selectivity. To this end, we studied the influence of the chelate ring size and the size of the alkyl substituent on the ligand and we also varied the metal.

The influence of ligand variations on the performance of [Ru(*p*-cym)(L)] complexes was investigated first. Syntheses of related [RuCp*(L)] complexes proved troublesome (vide infra), confirming the synthetic problems reported by Cross et al.[23] Additionally, ligand effects and structure–activity relations were more easily detected for somewhat slower catalysts, which was an additional reason why we focused on [Ru(*p*-cym)(L)] rather than [RuCp*(L)] complexes in our studies. For comparative investigations with iridium and rhodium we synthesized the Cp* analogues because the *p*-cym precursor was not accessible. To evaluate the potential of the NHC–amine motif, we investigated the performance of these types of catalysts on more challenging compounds: biomass-inspired model substrates, such as cinnamaldehyde, and actual platform chemicals, such as levulinic acid (LA) and hydroxymethyl furfural (HMF). Additionally, esters such as methyl butyrate (MB) or dimethyl oxalate (DMO) were tested. In doing so, we initiated broadening of the substrate scope of these NHC–amine complexes to include these platform chemicals. These substrates are of particular interest in the fine-chemical and pharmaceutical sector because they are all key building blocks or precursors for sustainable chemicals, materials, and biofuels.

Results and Discussion

Synthesis and characterization of ligands and catalysts

The ligands used were prepared according to the procedures shown in Scheme 1. 2-(2-Imidazolyl)aniline was obtained by an Ulmann-type coupling followed by hydrogenation of the nitro group. The imidazolium ligand precursors (**1**–**4**) were then obtained in good yields by *N*-alkylation in a sealed tube with the respective iodo- or bromoalkyl reagent. These were subsequently used to prepare the ruthenium complexes **6** and **9**–**11** (Scheme 1).

[Ru(*p*-cym)Cl(L)]PF_6 (**6**) was prepared from the isolated silver carbene precursor (**1a**), followed by reaction with the [Ru(*p*-cym)Cl_2]$_2$ precursor in the presence of a large excess of KPF_6 (route A). [Ru(*p*-cym)(ligand)]I complexes **9**–**11** were obtained in a one-pot reaction (route B) from **2**–**4**, but this route resulted in lower yields. The analogous IrCp* and RhCp* complexes were obtained in a similar manner following route A, using [IrCp*Cl]$_2$ and [RhCp*Cl_2]$_2$ as the metal precursors and yielding **7** and **8**, respectively. From complexes **6**–**8**, crystals that were suitable for crystallographic analysis were grown.[35] Complex **6** is shown in Figure 3 and complex **7**, which is isostructural with **8** and differs only in the disordered solvent molecules, is shown in Figure 4.

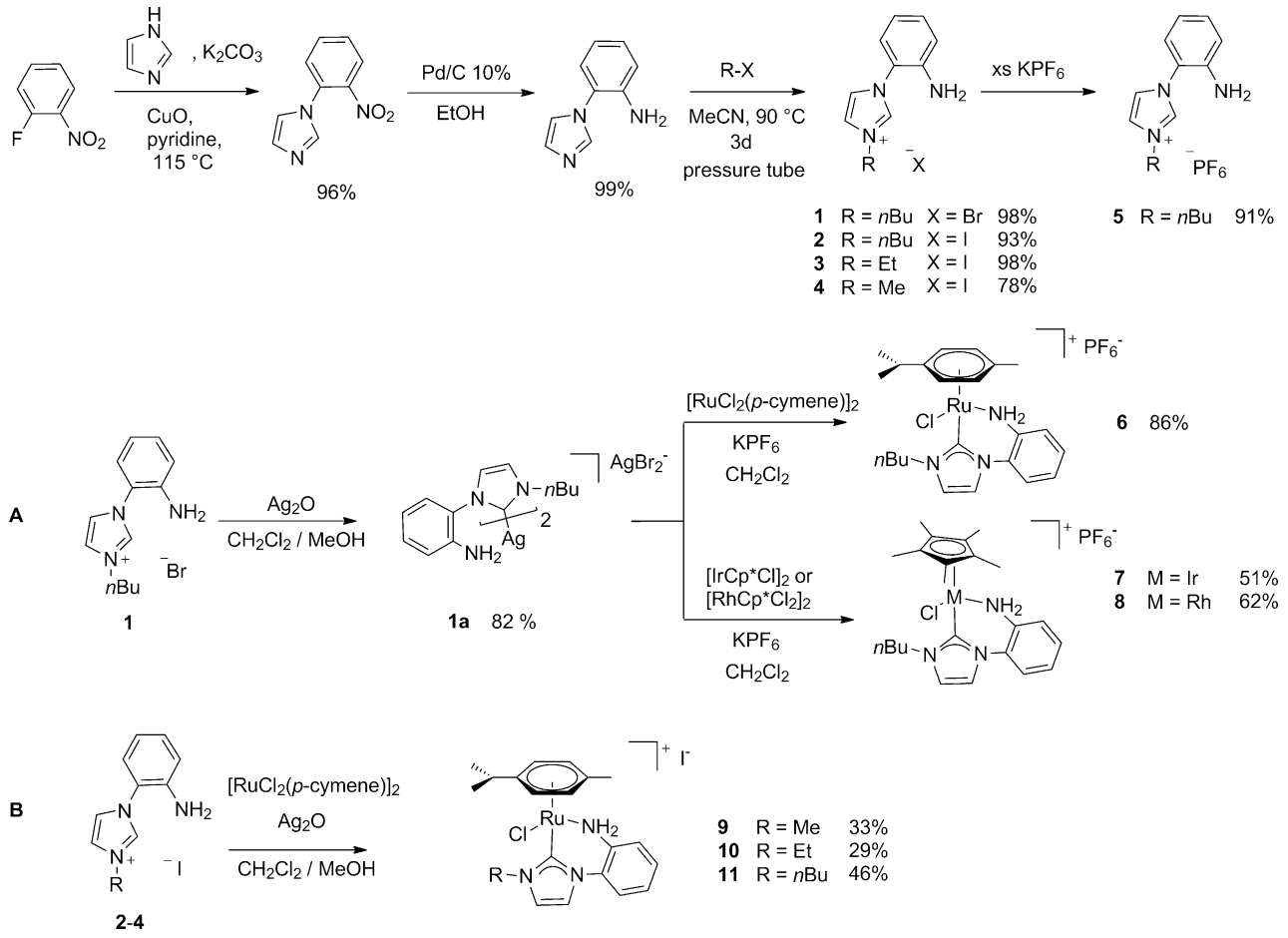

Scheme 1. Synthesis of the imidazolium ligands M–half-sandwich complexes through Route A and B.

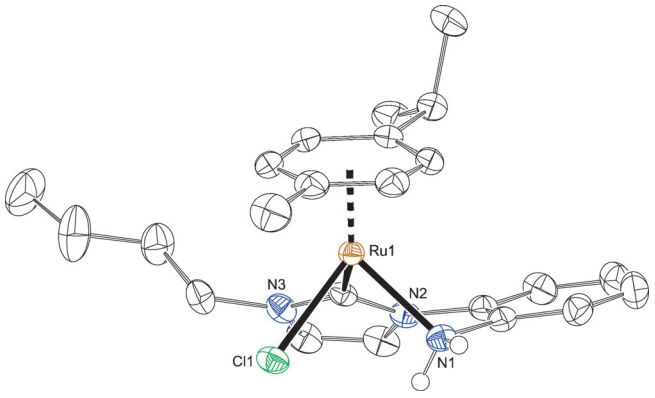

Figure 3. Displacement ellipsoid plot of [Ru(*p*-cym)Cl(L)]PF_6 (**6**) in the crystal, drawn at the 50% probability level. C–H hydrogen atoms and PF_6 anion are omitted for clarity. Only the major conformation of the disordered *n*-butyl group is shown.

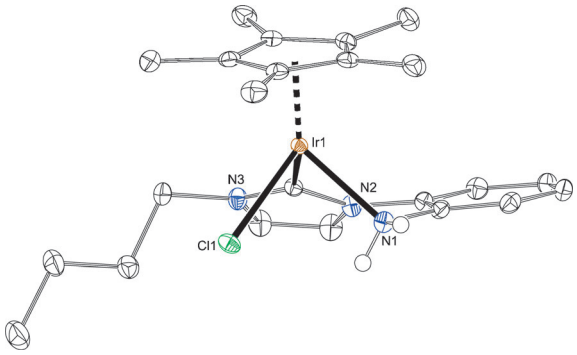

Figure 4. Displacement ellipsoid plot of [IrCp*Cl(L)]PF_6] (**7**) in the crystal, drawn at the 50% probability level. C–H hydrogen atoms, PF_6 anion, and disordered CH_2Cl_2 molecule are omitted for clarity.

Several attempts to synthesize the analogous [RuCp*(L)]Cl complex have proven unsuccessful. Unfortunately, using either NaH, KO*t*Bu, Ag_2O, or sodium hexamethyldisilazide (NaHMDS) as the base or using the appropriate silver complex for transmetallation of several metal precursors, such as $[RuCp^*(\mu_3\text{-}Cl)]_4$, $[RuCp^*Cl_2]_n$, and [RuCp*Cl(cod)] (cod = 1,5-cyclooctadiene), resulted in unidentifiable mixtures of products. Apparently, the RuCp* complex with a 6-membered NHC–aniline chelate ring was difficult to prepare and there are no reports of the synthesis of this or similar complexes. A likely reason for this behavior is the intrinsic reactivity of ruthenium towards the aromatic aniline ring. When stirring ligand **5** and the $[RuCp^*(\mu_3\text{-}Cl)]_4$ pre-

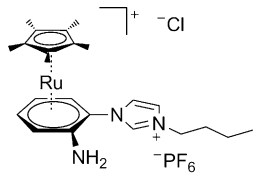

12

Figure 5. Proposed structure of RuCp* compound.

cursor in THF in the absence of base, a fine yellow precipitate formed. NMR experiments indicated formation of complex **12** (Figure 5). The chemical shifts of the aromatic ring of the ligand as detected in both ^{1}H and ^{13}C NMR spectra (around 5.5 and 80 ppm, respectively) were comparable to those reported for the aniline ligand in [RuCp*(η^6-aniline)]Cl.[29] The large downfield chemical shift of the amine protons in the ^{1}H NMR spectrum of **12** to 6.95 ppm, showing only coupling to itself in (^{1}H–^{1}H) correlation spectra (COSY) and no coupling to a carbon in (^{13}C–^{1}H) heteronuclear single quantum coherence (HSQC) NMR spectra, suggested that the amine protons became more acidic relative to the free ligand due to resonance of the amine lone pair with the π system of the aromatic ring. This readily explains the observed and undesired coordination mode. The RuCp* analogue containing a benzylic amine (general structure III) does not share this resonance structure, and hence, in contrast to **12**,[30] this complex is readily synthesized in its desired NHC coordination mode.

Structural parameters of the catalysts

We first analyzed the structural and spectroscopic differences between **6** (containing an aryl-derived six-membered chelate ring), and the analogous complexes **13** (containing an aliphatic six-membered chelate ring) and **14** (containing a benzylic seven-membered chelate ring) synthesized by Morris et al.[24,25] Several important properties related to the chelate ring size of these complexes are summarized in Table 1.

The influence of the *n*Bu group of **6** relative to the Me substituent in **13** and **14** is evaluated further on (vide infra).

The C–Ru–N bite angle in **6** is 79.62(6)°, which is significantly smaller than that in **13** and **14** (87.0 and 91.98°, respectively).[24,25] In the geometry of these complexes, the optimal angle of the chelate ring would be 90°, implying that complex **6** is somewhat strained. That causes a nonoptimal orbital overlap of the Ru–N bond, an important factor when an inner-sphere reaction mechanism requires dissociation of the amine. The carbene carbon of **6** resonates slightly downfield in ^{13}C NMR spectra relative to **13** and **14**, indicating a more electron-rich carbene. That correlates to the shorter Ru–C bond length, suggesting a stronger Ru–C interaction. A more electron-rich carbene means a more strongly donating NHC moiety, which is likely beneficial for hydrogenation. Using the aniline ligand with a conjugated system also renders the NHC group more electron rich. Assuming that the [Ru(*p*-cym)] complexes follow an inner-sphere route, the amine probably needs to dissociate from the metal center. This is promoted by a more strained system with a small chelating ring. The ^{13}C NMR carbene signals of complexes **9**–**11**, which differ in their alkyl substituents appear slightly further downfield at 178.21 (*n*Bu), 176.62 (Et), and 179.09 ppm (Me).

Table 1. Selected structural and spectroscopic parameters.[a]

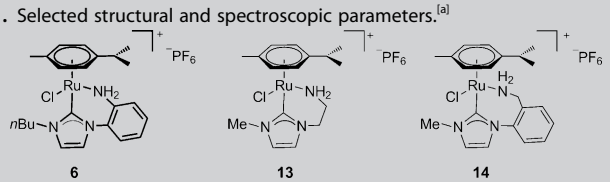

6 13 14

Complex	Bond length [Å]			Bond angle [°]	^{13}C NMR shift of
	$Ru–C_{carbene}$	Ru–N	Ru–Cl	carbene–Ru–N	carbene[b] [ppm]
6	2.0394(15)	2.1399(14)	2.3973(4)	79.62(6)	177.2
13	2.041(6)	2.114(4)	2.4140(15)	87.0(2)	174
14	2.092(5)	2.146(4)	2.4180(13)	91.98(17)	175.1

[a] Structural parameters of **6** obtained from the X-ray crystal structure. Structural parameters of **13** and **14** taken from Refs. [25] and [24]. [b] Carbene shift in CD_2Cl_2.

Catalytic hydrogenation experiments

We next evaluated the catalytic activity of complex **6** and compared the results with the activity reported for **13** and **14**.

As a benchmark reaction, the catalytic hydrogenation of acetophenone to 1-phenylethanol with H_2 in the presence of

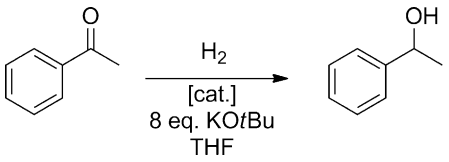

Scheme 2. Benchmark catalytic hydrogenation of acetophenone with H_2.

KO*t*Bu in THF was investigated (Scheme 2, Table 2). The TOFs increase with decreasing chelate ring size: **14** < **13** < **6** (Table 2, entries 6, 4, and 1, respectively). Additionally, increasing the substrate loading linearly increases the TOF (Table 2, entries 1–3, 548 vs. 1202 vs. 3609 h^{-1}). This activity is unprecedented for this type of half-sandwich NHC–amine complexes in this reaction. A linear dependence of the TOF with respect to substrate concentration was also observed for complex **13** (Table 2, entries 4 and 5, from 298 to 595 h^{-1}). Curiously, the opposite has been reported for complex **14**: an increase in substrate loading results in a decrease of the TOF.[26] To further investigate the effect of the chelate ring size, we turned our attention to the iridium and rhodium complexes **7** and **8** and the seven-membered-ring chelate iridium complex **15**.

Although the iridium systems are less active than the ruthenium catalyst, indeed a similar relation between the TOF and the chelate ring effect was observed for the IrCp* complexes **7** and **15** (Table 3, entries 8 and 9). For the even less active rhodium complex **8** (Table 3, entries 10 and 11) we have no comparison for the larger seven-membered-ring compound. Besides Cross et al.,[23] another related rhodium example containing a secondary amino-

Table 2. H_2 hydrogenation of acetophenone with Ru complexes of variable chelating ring size.

Entry[a]	Complex	C/B/S[b]	Reaction time [h]	Conversion[c] [%]	TOF[d] [h^{-1}]
1	**6**	1/8/100	0.5	99	548
2	**6**	1/8/200	0.5	99	1202
3	**6**	1/8/600	0.5	99	3609
4	**13**	1/8/200	1	99	298
5	**13**	1/8/600	2	99	595
6	**14**	1/8/200	2	99	213
7	**14**	1/8/600	2.5	57	122

[a] Reactions (Scheme 2) were carried out at 25 bar H_2 and at 50 °C in THF (15 mL) using KO*t*Bu as base. [b] C/B/S = catalyst/base/substrate ratio. [c] Conversions were determined by GC analysis using *p*-xylene as an internal standard. [d] Determined from the steepest part of the plot (between 40–60% conversion). Details for complexes **13**[25] and **14**[26] were taken from the literature.

Table 3. H_2 hydrogenation of acetophenone with iridium and rhodium complexes of variable chelating ring size.

Entry[a]	Complex	C/B/S[b]	Reaction time [h]	Conversion[c] [%]	TOF[d] [h^{-1}]
8	**7**	1/8/200	4	95	190
9	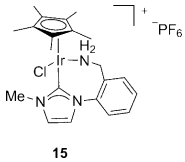 **15**	1/8/200	3	98	154
10	**8**	1/8/200	0	0	n.d.[e]
11[f]	**8**	1/8/200	3	98	n.d.[e]

[a] Reactions (Scheme 2) were carried out at 25 bar H_2 and at 50 °C in THF (15 mL) using KO*t*Bu as base. [b] C/B/S = catalyst/base/substrate ratio. [c] Conversions were determined by GC analysis using *p*-xylene as an internal standard. [d] Determined from the steepest part of the plot (between 40–60% conversion). [e] Not determined. [f] P_{H_2} = 50 bar. Details for complex **15** were taken from the literature.[28]

tethered NHC, [Rh(cod)(L)] [L = 1-Mes-3-(2-(Mes-NH)ethyl)imidazolium, Mes = 2,4,6-trimethylphenyl], was reported by Fryzuk et al.[31] This complex did not show any activity in hydrogenation of polar bonds at all and only alkene hydrogenation was reported. Complex **8** thus seems to be the first Rh/NHC–amine complex reported to be active in the direct hydrogenation of ketones.

The increased TOF for complexes containing ligand **1** can be explained by two contributing effects. (1) The smaller chelating ring size can account for a less tightly bound amine because the system is more strained. The aniline is also less basic than the benzyl amine and both factors could cause the amine to de-coordinate more readily, thereby promoting coordination of the substrate. (2) Additionally, the conjugated system renders the NHC more electron rich, thus making it a stronger donor. The first effect should be much less pronounced for the iridium systems because these Cp*-containing complexes most likely follow an (alcohol-assisted) outer-sphere mechanism, in which the amine remains coordinated and the substrate does not have to coordinate to the metal.[28]

Table 4. H_2-hydrogenation of acetophenone with complexes with varying alkyl substituents.

Entry[a]	Complex	C/B/S[b]	Conversion[c] [%]	TOF[d] [h^{-1}]
12	**9** (R = Me)	1/8/200	99	909
13	**10** (R = Et)	1/8/200	99	915
14	**11** (R = *n*Bu)	1/8/200	99	1543

[a] Reactions (Scheme 2) were carried out at 25 bar H_2 and at 50 °C, in THF (15 mL) using KO*t*Bu as base. [b] C/B/S = catalyst/base/substrate ratio. [c] Conversions were determined by GC analysis using *p*-xylene as an internal standard after 0.5 h reaction. [d] Determined from the steepest part of the plot (between 40–60% conversion) and as an average of two runs.

We further evaluated the influence of the *N*-alkyl substituent on the ligand by testing complexes **9**–**11** in the H_2 hydrogenation of acetophenone (Scheme 2, Table 4). Surprisingly, a substantial increase of the TOF was observed on going from Me/Et complexes (**9**/**10**) to the *n*Bu complex **11** (Table 4).

This effect is primarily caused by differences in catalyst activation rates. Inspection of the reaction profile reveals that the induction period for all complexes is different (Figure 6). At *t* = 0 the reaction mixture containing deprotonated complex and substrate is pressurized with H_2, forming the active species (Scheme 3). Going from *n*Bu to Me the induction period becomes much longer, clearly pointing to differences in the rates of formation of the active species in each case. The larger bulk of the *n*Bu group with respect to Me and Et substituents possibly influences the spatial positioning of the ligand in such a way that the amine is tilted into a position closer to the metal center, rendering the complex better suited for activation of the incoming dihydrogen reagent and thus leading to more efficient catalyst activation (Scheme 3).

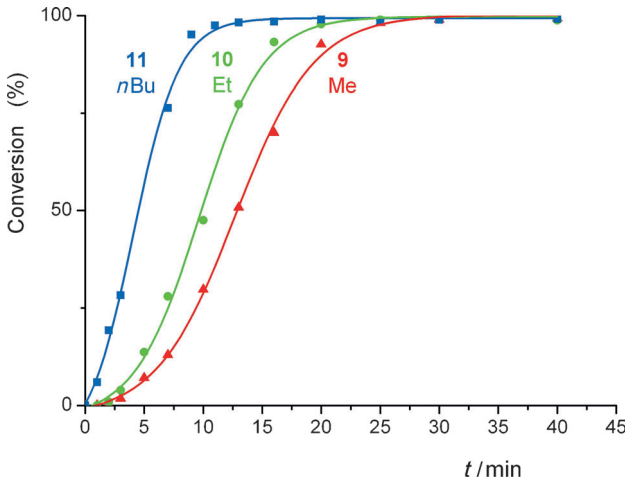

Figure 6. Performance in time of Ru(*p*-cym)Cl(L) complexes in the H_2-hydrogenation of acetophenone with varying alkyl substituents on the ligand: R = Me (red triangles), Et (green circles), *n*Bu (blue squares).

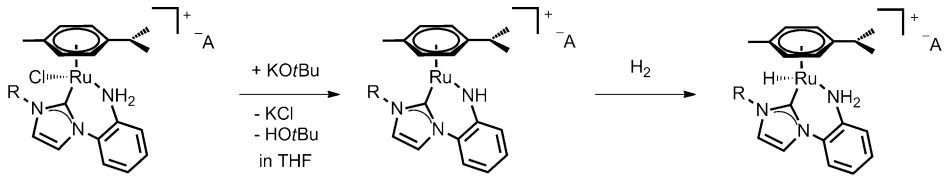

Scheme 3. Catalyst activation by amine deprotonation followed by (bifunctional) dihydrogen activation involving heterolytic splitting of H_2 over the M–amine bond leading to the proposed activated species.

Alternatively, there is a possibility that the ketone substrate coordinates to the deprotonated complex before formation of the active hydride species. The bulk of the *n*Bu group might help to push away the ketone substrate to allow the formation of the active hydride species by H_2.

The RuCp*Cl(η^6L) species (**12**) was also tested in a catalysis run. In absence of a coordinating electron-donating NHC the catalytic activity of this Ru sandwich species is low, converting 84% of acetophenone in 17 h at 50 °C and 25 bar H_2.

Conversion of platform chemicals and model compounds thereof

To further investigate the performance of **6**, several relevant types of biomass-inspired substrates have been subjected to hydrogenation. More challenging and with a higher degree of functionalization than acetophenone, these substrates are a good measure of the capacities of this type of NHC–amine-containing catalysts for application in biomass (Table 5). Using LA as substrate only minor conversion to the ring-closed product γ-valerolactone was observed (Table 5, entry 1a) probably due to incompatibility with the amine functionality of the catalyst. Upon mixing the deprotonated complex with this acid, a color change from brown to green was observed, showing that the conditions become acidic enough to protonate the amino functionality to form a different active species.[32] Increasing both temperature and pressure does improve conversion (Table 5, entry 1b), but increasing substrate loading (Table 5, entries 1c and b) does not. Applying methyl levulinate in hydrogenation also showed selective conversion of the ketone functionality (Table 5, entry 2). Again, higher temperatures and pressures than those used in the benchmark reaction with acetophenone were required, resulting in 86% conversion overnight. The lower activity might be attributed to competition between coordination of the ketone and the ester functionality. Linear ester functionalities, such as those in MB, are not converted by **6** (Table 5, entry 3). However, the conjungated diester DMO, in which one ester functionality activates the other one for hydrogenation, is converted slowly (29% conversion in 24 h) to methyl 2-hydroxyacetate (Table 5, entry 4). The highly functionalized aldehyde HMF is converted to the bishydroxy compound furan-2,5-diyldimethanol in 2 h at 70 °C and 50 bar H_2 (Table 5, entry 5). Application of the α,β-unsaturated compound cinnamaldehyde is a good measure for the selectivity of the catalyst. After 6 h at an elevated temperature and pressure, a roughly 50:50 product distribution of the hydrogenated ketone and the completely hydrogenated product was detected. The latter is probably formed by hydrogenation of the hydrocinnamaldehyde intermediate, which is only present in trace amounts throughout the entire reaction (Table 5, entry 6).

Table 5. Biomass-inspired substrates tested in H_2 hydrogenation using **6** as catalyst.

Entry[a]	Substrate	Conditions		Product	Reaction time [h]	Conversion[b] [%]
		T [°C]	P_{H_2} [bar]			
1a	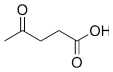	50	25		17	15
1b		70	50		17	85
1c[c]		70	50		17	15
1d[d]		70	50		17	35
2	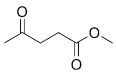	70	50		17	86
3[e]		80	80		17	0
4		80	80		24	29
5	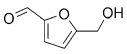	70	50	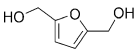	2	99
6		70	50		6 24	47/2/38 8/0/90

[a] Reactions were carried out at 25 bar H_2 and at 50 °C in THF (15 mL) using KO*t*Bu as base and complex **6** as catalyst; C/B/S = 1/8/200. [b] Conversions were determined by GC analysis using *p*-xylene as an internal standard. [c] C/B/S = 1/8/2000 in THF (2 mL). [d] C/B/S = 1/8/1000. [e] C/B/S/ = 1/8/600.

Conclusions

We have shown that half-sandwich complexes with an amino-tethered NHC, most notably ruthenium complexes, show good activity in hydrogenation of polar functionalities. Acetophenone is hydrogenated by [Ru(*p*-cym)Cl(L)]A (**6**, **9**–**11**) which most probably proceeds through an inner-sphere mechanism, showing excellent activity with TOFs as high as 3600 h^{-1} for complex **6**. We are also the first to report a Rh/NHC–amine species of this type to be active in the direct hydrogenation of ketones. The activity of this type of catalyst is greatly influenced by the type of chelating ligand and the N-substituent on the NHC. A conjugating, small chelate ring is beneficial for the activity. Also, a larger

alkyl substituent on the NHC promotes the formation of the active species and thereby greatly reduces the induction period. The applicability of complex **6** is successfully extended to key biomass-derived substrates. Functionalized aldehydes, ketones, and activated diesters have been converted readily at moderate pressures and temperatures (50 bar H_2, 70 °C).

Our study has provided more thorough knowledge concerning the workings of NHC–amine complexes of Ru, Ir, and Rh in direct hydrogenation of polar functionalities, which will aid the future rational design of hydrogenation catalysts for the conversion of biomass into useful/added-value compounds.

Experimental Section

General remarks, detailed experimental procedures (to obtain the reported ligands **1**–**5**, the silver carbene **1 a** in Scheme 1, and complex **12**), and crystallographic data of complexes **6**–**8** can be found in the Supporting Information.

Complex synthesis

[Ru(*p*-cym)Cl(*n*Bu–C^{NHC}–NH_2)]PF_6 (**6**): A solution of **1 a** (0.27 g, 0.66 mmol) in CH_2Cl_2 (15 mL) was added to a solution of [$RuCl_2$(*p*-cym)]$_2$ (0.19 g, 0.30 mmol) and KPF_6 (0.36 g, 1.98 mmol) in CH_2Cl_2 (20 mL), and the mixture was stirred at RT for 3 h, during which the solution became dark green with grey silver halides suspended in it. The mixture was filtered over a pad of Celite and the volume of filtrate was reduced to 3 mL. Pentane (20 mL) was added, which resulted in a precipitation of a dark green solid. Repeated precipitation from CH_2Cl_2 with Et_2O furnished the desired light green complex (0.19 g, 96%). ^{1}H NMR (300 MHz, CD_2Cl_2): δ = 7.74 (d, J = 6.7 Hz, 1H, =C*H*), 7.65 (d, J = 2.2 Hz, 1H, =C*H*), 7.42 (m, 4H, H_{Ar}), 6.52 (d, J = 8.9 Hz, 1H, NH_2), 5.83 (d, J = 5.9 Hz, 1H, H_{Ar} *p*-cym), 5.71 (d, J = 6.1 Hz, 1H, H_{Ar} *p*-cym), 5.09 (m, 2H, H_{Ar} *p*-cym), 4.38 (d, J = 10.6 Hz, 1H, NH_2), 4.29 (t, J = 8.1 Hz, 2H, NCH_2), 2.05–1.80 (m, 3H, CH_2 and C*H* *p*-cym), 1.74 (s, 3H, CH_3 *p*-cym), 1.52 (m, 2H, CH_2), 1.05 (t, J = 7.3 Hz, 3H, CH_3), 0.93 ppm (dd, J = 16.6, 6.9 Hz, 6H, CH_3 *i*Pr); ^{13}C NMR (75 MHz, CD_2Cl_2): δ = 177.22, 134.26, 132.06, 128.80, 127.68, 123.71, 121.75, 120.14, 109.37, 101.81, 89.06, 83.89, 83.73, 81.96, 51.52, 33.01, 30.78, 23.33, 20.19, 19.85, 17.83, 13.62, 0.74 ppm; ^{31}P NMR (121 MHz, CD_2Cl_2): δ = −144.06 ppm (septet, J = 711.9 Hz); ^{19}F NMR (282 MHz, CD_2Cl_2): δ = −70.14 ppm (d, J = 711.1 Hz); FAB^+–MS (CH_2Cl_2) (FAB: fast atom bombardment mass spectrometry): calcd for $C_{23}H_{31}ClN_3Ru$+PF_6^-: *m*/*z* calcd 486.1253 (100%) [M–PF6$^-$]$^+$, found 486.1248.

[IrCp*Cl(*n*Bu–C^{NHC}–NH_2)] PF_6 (**7**): [IrCp*Cl]$_2$ (0.25 mmol, 199 mg) and KPF_6 (1.25 mmol, 230 mg) in 8 mL CH_2Cl_2 was added to a solution of **1 a** (201 mg, 0.25 mmol) in CH_2Cl_2 (7 mL) and stirred at RT under the exclusion of light for 2 h. The resulting reaction mixture was filtered over a pad of Celite, and the solvent was evaporated in vacuo. The complex was purified by dissolution in a CH_2Cl_2/Et_2O mixture (7 mL; 2:5 *v*/*v*) and cooling to 4 °C to obtain **7** in a crystalline form in 51% yield. ^{1}H NMR (300 MHz, CD_2Cl_2): δ = 7.70 (d, J = 2.2 Hz, 1H, =C*H*), 7.54 (m, 2H, H_{Ar}), 7.49–7.40 (m, 2H, H_{Ar}), 7.38 (d, J = 2.2 Hz, 1H, =C*H*), 6.12 (bs, 2H, NH_2), 4.26 (m, 1H, NCH_2), 3.97 (m, 1H, NCH_2), 1.88 (m, 2H, CH_2), 1.46 (s, 17H, Cp*–CH_3 and CH_2), 1.01 ppm (t, J = 7.4 Hz, 2H, CH_3); ^{13}C NMR (75 MHz, CD_2Cl_2): δ = 160.97, 133.81, 132.54, 128.12, 127.89, 122.87, 122.82, 121.84, 121.66, 119.71, 90.13, 50.81, 33.21, 20.03, 13.59, 8.13 ppm; ^{19}F NMR (282 MHz, CD_2Cl_2): δ = −72.06 ppm (d, J = 711.7 Hz); FAB^+–MS: $C_{23}H_{32}ClN_3Ir$: *m*/*z* calcd 578.1907 (100%) [M–PF_6^-]$^+$, found 578.1907.

[RhCp*Cl(*n*Bu–C^{NHC}–NH_2)] PF_6 (**8**): [RhCp*Cl_2]$_2$ (0.095 mmol, 59 mg), KPF_6 (175 mg, 0.95 mmol), and **1 a** (77 mg, 0.19 mmol) were weighed in a Schlenk tube and dissolved in CH_2Cl_2 (10 mL). The solution was stirred at RT for 24 h under the exclusion of light. The mixture was then filtered over a pad of Celite, and the solvent was evaporated in vacuo (to a volume of 1 mL) and precipitated with Et_2O. The complex was purified by dissolution in a THF/pentane mixture (8 mL; 1:3 *v*/*v*) and cooling to 4 °C to obtain **8** in a crystalline form in 62% yield. ^{1}H NMR (300 MHz, CD_2Cl_2): δ = 7.73 (d, J = 2.2 Hz, 1H, =C*H*), 7.57–7.42 (m, 4H, H_{Ar}), 7.45 (d, J = 2.4 Hz, 1H, =C*H*), 5.19 (bs, 2H, NH_2), 4.26 (m, 1H, NCH_2), 4.02 (m, 1H, NCH_2), 1.87 (m, 2H, CH_2), 1.42 (s, 17H, Cp*–CH_3–and CH_2), 1.02 ppm (t, J = 7.4 Hz, 2H, CH_3); ^{13}C NMR (75 MHz, CD_2Cl_2): δ = 173.02 (d, J = 53 Hz, N_2C–Rh), 133.12, 132.11, 128.46, 127.57, 123.63, 122.32, 121.84, 120.98, 97.62 (d, J = 98, η^5-C_5Me_5), 51.04, 32.79, 20.03, 13.57, 8.34 ppm; ^{19}F NMR (282 MHz, CD_2Cl_2): δ = −72.19 ppm (d, J = 711.9 Hz); FAB^+-MS: $C_{23}H_{32}ClN_3Rh$: *m*/*z* calcd 488.1340 (100%) [M–PF_6^-]$^+$, found 488.1335; elemental analysis calcd (%) for $C_{23}H_{32}ClF_6N_3PRh$: C 43.58, H 5.0, N 6.63, found: C 42.15, H 4.97, N, 6.49.

[Ru(*p*-cym)Cl(R–C^{NHC}–NH_2)][I] (**9**–**11**) (based on a modified procedure from Ref. [23]): [Ru(*p*-cym)Cl_2]$_2$ (97 mg, 0.16 mmol), the appropriate imidazolium salt (**2**–**4**) (0.32 mmol), and Ag_2O (37 mg, 0.16 mmol) were weighed in a Schlenk tube, dissolved in CH_2Cl_2 (15 mL), and stirred under absence of light at 33 °C overnight. The solvent was then removed in vacuo; KI (0.53 gr, 3.17 mmol) was added to the residue, and the mixture was redissolved in acetone (20 mL) and stirred at reflux for 1 h. The solvent was removed in vacuo, the crude product redissolved in CH_2Cl_2 (20 mL), filtered over Celite pad, and concentrated under vacuum. The complex was purified by repeatedly dissolving in a CH_2Cl_2/Et_2O mixture and cooling to 4 °C to obtain the pure complex.

Spectral data for **9** (R = Me): Complex **9** was obtained as a dark brown crystalline solid in 33% yield. ^{1}H NMR (300 MHz, CD_2Cl_2): δ = 10.08 (d, J = 9.9 Hz, 1H, NH_2), 8.60 (d, J = 6.8 Hz, 1H, H_{Ar}), 7.62 (s, 1H, =C*H*), 7.36 (s, 1H, H_{Ar}), 7.42–7.18 (m, 3H, H_{Ar}), 6.24 (d, J = 5.4 Hz, 1H, H_{Ar} *p*-cym), 5.85 (d, J = 5.7 Hz, 1H, H_{Ar} *p*-cym), 5.32 (d, J = 5.4 Hz, 1H, H_{Ar} *p*-cym), 5.19 (d, J = 5.7 Hz, 1H, H_{Ar} *p*-cym), 4.06 (s, 1H, NH_2), 4.01 (s, 3H, CNH_3), 1.90 (m, 1H, C*H* *p*-cym), 1.77 (s, 3H, CH_3 *p*-cym), 0.86 ppm (dd, J = 19.8, 6.8 Hz, 6H, CH_3 *i*Pr); ^{13}C NMR (75 MHz, CD_2Cl_2): δ = 179.09, 155.58, 155.44, 135.61, 132.53, 128.26, 126.85, 125.78, 123.72, 120.98, 119.41, 107.37, 102.08, 89.87, 83.89, 83.11, 30.62, 23.35, 20.15, 18.00 ppm.

Spectral data for **10** (R = Et). Complex **10** was obtained as a brown microcrystalline powder in 29% yield. ^{1}H NMR (300 MHz, CD_2Cl_2): δ = 8.81–8.63 (m, 1H, H_{Ar}), 8.56 (d, J = 11.2 Hz, 1H, NH_2), 7.77 (d, J = 2.2 Hz, 1H, =C*H*), 7.46 (d, J = 2.1 Hz, 1H, =C*H*), 7.37 (dt, J = 6.8, 4.0 Hz, 3H, H_{Ar}), 6.31 (d, J = 6.0 Hz, 1H, H_{Ar} *p*-cym), 5.79 (d, J = 6.0 Hz, 1H, H_{Ar} *p*-cym), 5.22 (dd, J = 10.5, 6.1 Hz, 2H, H_{Ar} *p*-cym), 4.33 (ddq, J = 35.5, 14.6, 7.4 Hz, 2H, NCH_2), 4.17 (d, J = 11.3 Hz, 1H, NH_2), 2.14 (m, 1H, C*H* *p*-cym) 2.09 (s, 3H, CH_3 *p*-cym), 1.58 (t, J = 7.3 Hz, 3H, CH_3), 0.92 ppm (dd, J = 6.9, 4.1 Hz, 6H, CH_3 *i*Pr); ^{13}C NMR (75 MHz, CD_2Cl_2): δ = 176.62, 135.80, 132.57, 128.22, 127.28, 123.13, 122.39, 121.57, 120.53, 110.48, 102.22, 89.51, 84.02, 82.76, 82.22, 48.61, 31.50, 23.67, 20.44, 19.75, 15.69 ppm.

Spectral data for **11** (R = *n*Bu). Complex **11** was obtained in a dark brown microcrystalline solid in 46% yield. ^{1}H NMR (300 MHz, CD_2Cl_2): δ = 10.14 (bs, 1H, NH_2), 8.57 (s, 1H, =C*H*), 7.72 (s, 1H, =C*H*), 7.36 (m, 4H, H_{Ar}), 6.16 (d, J = 5.5 Hz, 1H, H_{Ar} *p*-cym), 5.81 (d, J = 5.9 Hz, 1H, H_{Ar} *p*-cym), 5.28 (d, J = 5.5 Hz, 1H, H_{Ar} *p*-cym), 5.18 (d,

J = 5.8 Hz, 1H, H_{Ar} *p*-cym), 4.31 (t, J = 7.1 Hz, 2H, NCH_2), 4.01 (bs, J = 9.1 Hz, 1H, NH_2), 1.91 (m, 3H, $CH_2 + CH$ *p*-cym), 1.50 (m, J = 7.4 Hz, 2H, CH_2), 1.03 (t, J = 7.3 Hz, 3H, CH_3), 0.87 ppm (dd, J = 25.8, 6.9 Hz, 6H, CH_3 *i*Pr); ^{13}C NMR (75 MHz, CD_2Cl_2): δ = 178.21, 135.78, 132.57, 128.10, 126.90, 123.58, 123.14, 121.36, 120.18, 107.75, 101.25, 89.54, 84.20, 83.89, 51.48, 33.10, 30.58, 23.37, 20.23, 17.90, 13.70 ppm.

Hydrogenation experiments

Catalyst (0.014 mmol) and KO*t*Bu (0.12 mmol) were weighed in a Schlenk flask, dissolved in THF (15 mL), and let to stir for 30 min to ensure formation of the deprotonated complex. The appropriate amount of substrate and *p*-xylene (internal standard, 1.4 mmol) were then added. A homebuilt stainless-steel autoclave with a volume of 200 mL was flushed three times with N_2, and the mixture was inserted into the autoclave under a flow of N_2. The autoclave was then heated until the desired temperature (50–80 °C) was reached, flushed three times with H_2, and filled with the appropriate pressure of H_2 (25–80 bar H_2). If the reaction was monitored with regard to time, samples were taken through a sample port (first aliquot was discarded). After the reaction, the autoclave was cooled to RT with an ice bath and H_2 was vented carefully. The products were determined by GC analysis with *p*-xylene as internal standard, using a Thermo Scientific Trace GC Ultra system with a Restek RTX-200 (30 m, 0.25 mm inner diameter) capillary column with a split injecting method.

Acknowledgements

This research has been performed within the framework of the CatchBio program. The authors gratefully acknowledge the support of the Smart Mix Program of the Netherlands Ministry of Economic Affairs and the Netherlands Ministry of Education, Culture, and Science. The X-ray diffractometer has been financed by the Netherlands Organization for Scientific Research (NWO).

Keywords: bifunctional ligand · biomass · hydrogenation · rhodium · ruthenium

[1] A. J. Ragauskas, C. K. Williams, B. H. Davison, G. Britovsek, J. Cairney, C. A. Eckert, W. J. Frederick, Jr., J. P. Hallett, D. J. Leak, C. L. Liotta, J. R. Mielenz, R. Murphy, R. Templer, T. Tschaplinski, *Science* **2006**, *311*, 484–489.
[2] G. W. Huber, A. Corma, *Angew. Chem.* **2007**, *119*, 7320–7338; *Angew. Chem. Int. Ed.* **2007**, *46*, 7184–7201.
[3] J. N. Chheda, G. W. Huber, J. A. Dumesic, *Angew. Chem.* **2007**, *119*, 7298–7318; *Angew. Chem. Int. Ed.* **2007**, *46*, 7164–7183.
[4] T. Werpy, G. Petersen, J. E. Holladay, A. Aden, J. J. Bozell, J. F. White, D. Johnson, A. Manheim, *Top Value Added Chemicals from Biomass*, *Vol. I*, http://www1.eere.energy.gov/bioenergy/pdfs/35523.pdf, **2004**.
[5] F. M. A. Geilen, B. Engendahl, A. Harwardt, W. Marquardt, J. Klankermayer, W. Leitner, *Angew. Chem.* **2010**, *122*, 5642–5646; *Angew. Chem. Int. Ed.* **2010**, *49*, 5510–5514.
[6] F. M. A. Geilen, B. Engendahl, M. Hölscher, J. Klankermayer, W. Leitner, *J. Am. Chem. Soc.* **2011**, *133*, 14349–14358.
[7] S. D. Lacroix, A. Pennycook, S. Liu, T. T. Eisenhart, A. C. Marr, *Catal. Sci. Technol.* **2012**, *2*, 288.
[8] D. Gnanamgari, E. L. O. Sauer, N. D. Schley, C. Butler, C. D. Incarvito, R. H. Crabtree, *Organometallics* **2009**, *28*, 321–325.
[9] F. Hanasaka, K. Fujita, R. Yamaguchi, *Organometallics* **2006**, *25*, 4643–4647.
[10] A. Azua, J. A. Mata, E. Peris, F. Lamaty, J. Martinez, E. Colacino, *Organometallics* **2012**, *31*, 3911–3919.
[11] *The Handbook of Homogeneous Hydrogenation* (Eds.: J. G. de Vries, C. J. Elsevier), Wiley-VCH, Weinheim, **2006**.
[12] S. Hashiguchi, J. Takehara, T. Ikariya, R. Noyori, *J. Am. Chem. Soc.* **1995**, *117*, 7562–7563.
[13] A. Hadzovic, D. Song, C. M. MacLaughlin, R. H. Morris, *Organometallics* **2007**, *26*, 5987–5999.
[14] R. Noyori, C. A. Sandoval, K. Muñiz, T. Ohkuma, *Philos. Trans. R. Soc. A* **2005**, *363*, 901–912; discussion 1035–1040.
[15] M. Yamakawa, H. Ito, R. Noyori, *J. Am. Chem. Soc.* **2000**, *122*, 1466–1478.
[16] W. W. N. O, R. H. Morris, *ACS Catal.* **2013**, *3*, 32–40.
[17] M. L. Clarke, *Catal. Sci. Technol.* **2012**, *2*, 2418–2423.
[18] D. Milstein, *Top. Catal.* **2010**, *53*, 915–923.
[19] S. Díez-González, N. Marion, S. P. Nolan, *Chem. Rev.* **2009**, *109*, 3612–3676.
[20] M. Watanabe, Y. Kashiwame, S. Kuwata, T. Ikariya, *Eur. J. Inorg. Chem.* **2012**, 504–511.
[21] T. Ikariya, I. D. Gridnev, *Chem. Rec.* **2009**, *9*, 106–123.
[22] W. B. Cross, C. G. Daly, R. L. Ackerman, I. R. George, K. Singh, *Dalton Trans.* **2011**, *40*, 495–505.
[23] W. B. Cross, C. G. Daly, Y. Boutadla, K. Singh, *Dalton Trans.* **2011**, *40*, 9722–9730.
[24] W. W. N. O, A. J. Lough, R. H. Morris, *Organometallics* **2009**, *28*, 6755–6761.
[25] H. Ohara, W. W. N. O, A. J. Lough, R. H. Morris, *Dalton Trans.* **2012**, *41*, 8797–8808.
[26] W. W. N. O, A. J. Lough, R. H. Morris, *Organometallics* **2011**, *30*, 1236–1252.
[27] W. W. N. O, A. J. Lough, R. H. Morris, *Organometallics* **2012**, *31*, 2137–2151.
[28] W. W. N. O, A. J. Lough, R. H. Morris, *Organometallics* **2012**, *31*, 2152–2165.
[29] R. M. Fairchild, K. T. Holman, *Organometallics* **2007**, *26*, 3049–3053.
[30] W. W. N. O, A. J. Lough, R. H. Morris, *Chem. Commun.* **2010**, *46*, 8240–8242.
[31] H. Jong, B. O. Patrick, M. D. Fryzuk, *Can. J. Chem.* **2008**, *86*, 803–810.
[32] C. A. Sandoval, T. Ohkuma, N. Utsumi, K. Tsutsumi, K. Murata, R. Noyori, *Chem. Asian J.* **2006**, *1*, 102–110.
[33] A. J. Blake, B. a. J. Clark, H. McNab, C. C. Sommerville, *J. Chem. Soc. Perkin Trans. 1* **1997**, 1605–1608.
[34] P. J. Fagan, M. D. Ward, J. C. Calabrese, *J. Am. Chem. Soc.* **1989**, *111*, 1698–1719.
[35] CCDC 931590 (compound **6**), CCDC 931591 (compound **7**), and CCDC 931592 (compound **8**) contain the supplementary crystallographic data for this paper. These data can be obtained free of charge from The Cambridge Crystallographic Data Centre via www.ccdc.cam.ac.uk/data_request/cif.

Received: April 19, 2013
Revised: June 21, 2013

Part of a Special Issue on "CatchBio". To view the complete issue, visit:
http://onlinelibrary.wiley.com/doi/10.1002/cssc.v6.9/issuetoc